

# Integration of Leaky Waveguide Detection with Electrowetting on Dielectric Digital Microfluidic Devices

Ruchi Gupta<sup>1</sup> and Nick Goddard

School of Chemical Engineering and Analytical Science, University of Manchester,  
Oxford Road, Manchester M13 9PL, United Kingdom

Email: [ruchi.gupta@manchester.ac.uk](mailto:ruchi.gupta@manchester.ac.uk)

**Abstract.** Typically, Electrowetting on dielectric (EWOD) digital microfluidic devices consist of an array of metal electrodes covered with a continuous hydrophobic dielectric layer. The monitoring of droplet position and detection in EWOD is usually achieved via microscopy, thereby resulting in increasing the size and complexity of the instrumentation associated with such devices. This work for the first time demonstrates that metal clad leaky waveguide (MCLW) is suitable for detection in EWOD devices. MCLW devices typically consist of a metal layer covered with a dielectric layer in which the leaky waveguide mode propagates. The two structures are fundamentally compatible provided the metal and dielectric layer thicknesses and refractive indices can be optimised to permit both electrowetting and waveguiding. In this work, it has been shown that titanium electrodes covered with a fluoropolymer layer can be used to perform MCLW detection of droplets on EWOD platforms.

## 1. Introduction

Electrowetting on dielectric (EWOD) devices are attractive for a range of applications as a result of their programmability and portability [1-5]. Optical detection, typically based on microscopy [5-6] and transmission [7], is commonly used to measure the output (e.g. antibody-antigen interactions) and monitor the position of droplets within EWOD devices. Such detection methods necessitate that the electrodes on at least one side of the EWOD device are made from a transparent material such as Indium Tin Oxide (ITO). The use of transmission based detection methods also requires a "clean" (e.g. non-turbid or non-absorbing) sample. Surface Plasmon Resonance imaging (SPRi) [8], whispering gallery mode (WGM) resonators [9] and integrated waveguides [10] have also been used to perform label-free sensing within EWOD devices. The use of SPRi for detection within EWOD devices, however, requires the formation of local detection zones that are free of hydrophobic dielectric [8]. The use of the WGM resonator and integrated waveguides also require additional fabrication steps.

A typical metal clad leaky waveguide (MCLW) device consists of a dielectric waveguide and metal layers on a glass substrate. In a MCLW, Fresnel reflection is used at one waveguide boundary to partially confine light and a peak (or dip) in reflectivity is observed around the resonance angle. The shifts in the position and intensity of the peak (or dip) has been used to perform refractive index sensing and absorption measurements respectively [11-12]. To the best of our knowledge, however, the suitability of MCLW for detection within EWOD devices has not been reported.

---

<sup>1</sup> To whom all correspondence should be addressed



In this work, the inherent similarity of MCLW and EWOD structures has, for the first time, been exploited to perform detection and actuation using the same structure (See Figure 1 (a)). This reduces the complexity of fabrication and the integration of the EWOD device with optical instrumentation. In addition, MCLW devices can provide greater sensitivity than microscopy-based detection and relax the requirements for non-turbid and non-absorbing samples.

## 2. Experimental

### 2.1. Chemicals and Materials

The chemicals used are as follows: hydrogen peroxide (30%), sulphuric acid (98%), acetone (>99.9%), glycerol (>99%), titanium (>99.99%, all: Sigma-Aldrich, Gillingham, UK), Norland optical adhesive (NOA) 13685 (Tech Optics, Kent, UK), Teflon<sup>®</sup> AF 1600 (DuPont, Geneva, Switzerland), Fluorinert<sup>™</sup> FC-40 (3M, Bracknell, UK), SPR<sup>™</sup> 220-7.0 and MF-26A (both: Dow, Middlesbrough, UK). 18.2 MΩ water (Elga Maxima Ultra Pure, Vivendi Water Systems, Buckinghamshire, UK) was used. 1.2 mm thick glass slides were purchased from VWR International (Leicestershire, UK).

### 2.2. Microfabrication

#### 2.2.1. Fabrication of MCLW devices

The glass slides were cleaned in piranha solution (H<sub>2</sub>O<sub>2</sub>:H<sub>2</sub>SO<sub>4</sub>=1:3 (v:v)) and dried in an oven at 110 °C for 1 hour. The cleaned glass slides were cut into 25 mm×25 mm squares using a diamond scribe.

These squares were loaded into an electron beam deposition system (Auto500, Edwards, West Sussex, UK) to deposit 9 nm thick titanium at a rate of 0.2 nm/s and under a pressure of 10<sup>-6</sup> mbar. Film thickness was monitored by a quartz crystal oscillator (FTM7, Edwards, West Sussex, UK).

Other cleaned glass squares were spin coated with SPR<sup>™</sup> 220-7.0 at 5000 rpm for 30 s, baked at 110°C for 90 s on a hot plate and exposed for 62 s using a maskless photolithography system (SF-100, Intelligent Micro Patterning, Florida, USA). The resist coated slides were developed in MF-26A, rinsed in water and baked at 110°C for 30 min. 9 nm thick titanium was then deposited by following the procedure described above. Subsequently, the resist was removed using acetone to obtain rectangles of different size of titanium on the glass slides. The size of the titanium rectangles investigated in this work was 0.36 mm×0.48 mm, 0.72 mm×0.96 mm and 1.44 mm×1.92mm.

Unless stated otherwise, NOA 13685 was spin coated on the slides with continuous and patterned titanium layers at a speed of 2000 rpm for 30 s. The substrates were UV-cured (2000-EC UV curing flood lamp, Dymax, Germany) under nitrogen dust for 10 min. Finally, a solution of 1% Teflon<sup>®</sup> AF 1600 in Fluorinert<sup>™</sup> FC-40 was spin coated at 5000 rpm, 30 s and cured at 110°C for 30 min.

#### 2.2.2. Fabrication of MCLW integrated EWOD devices

The lower plate of EWOD devices was fabricated by depositing patterned titanium electrodes using the lift-off photolithography process described above. The contact pads were protected using tape. NOA 13685 was then spin coated at 2000 rpm, 30 s and UV-cured under nitrogen for 10 min. Subsequently, Teflon<sup>®</sup> AF 1600 was spin coated at 5000 rpm, 30 s and cured at 110 °C for 30 min to form a hydrophobic layer. The tape was then removed from the contact pads and wires were bonded using silver-loaded epoxy (RS components, Northamptonshire, UK). The upper plate was constructed in a similar way on a continuous titanium layer, but without the deposition of NOA 13685. A double-sided adhesive with a thickness of 275 μm (3M 467MP, Viking Industrial Products Ltd, Keighley, UK) was used as a spacer between the upper and lower plates.

### 2.3. Instrumentation

The optical set-up used to probe MCLW devices is shown in Figure 1 (b). A prism made of N-BK7 (Qioptic Photonics, Denbighshire, UK) was used to couple light into the device. The angular position of the light source and the detector were controlled by mounting them on rails, which were connected

to goniometers. A polystyrene flow cell was clamped firmly on top of the MCLW device, following which solutions were pumped using a peristaltic pump (Minipuls<sup>®</sup> 3, Gilson, Bedfordshire, UK) at a flow rate of 0.2 ml/min.

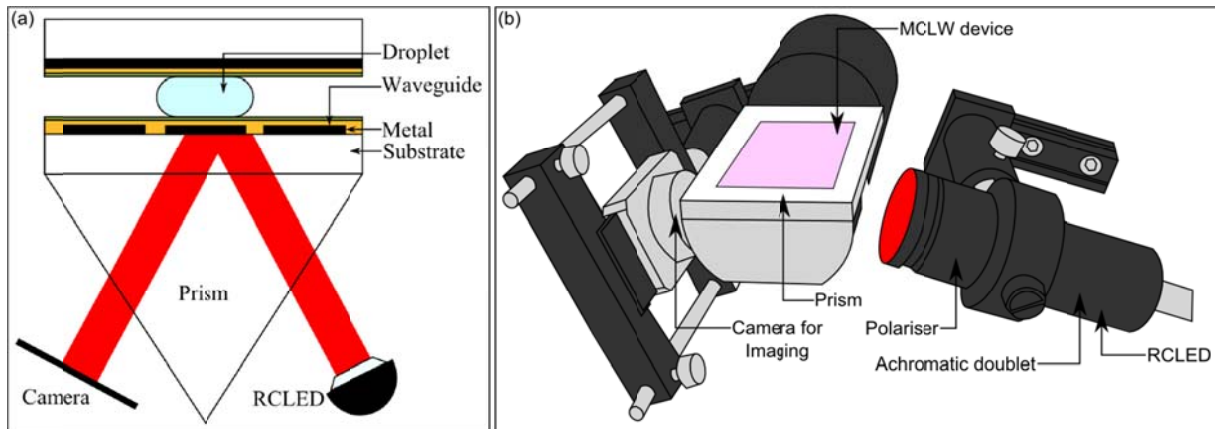


**Figure 1: A schematic of (a) MCLW with EWOD (b) optical set-up (the flow cell is not shown)**

Preliminary studies were performed using a TE-polarised laser (RS Components, Northamptonshire, UK) with a peak wavelength of 650 nm and a photodiode (Centronic, Surrey, UK).

In order to study the refractive index sensitivity of the MCLW device, a resonant cavity light emitting diode (RCLED, PR65-F1P0T, Roithner Lasertechnik, Vienna, Austria) was used. The light emitted from the RCLED was collimated and TE-polarised using an achromatic doublet (63 DQ 25) and polariser (32 CA 25, both: Comar Instruments, Cambridge, UK) respectively. A cylindrical lens was then placed in the path of light to obtain a beam with a wedge angle of  $\sim 34.7^\circ$  in air and  $\sim 21.1^\circ$  in N-BK7. The angle of the RCLED was fixed at  $72^\circ$  to obtain the peak at the centre of the image sensor. The output of the MCLW device *versus* time as different concentrations of glycerol solutions were introduced in the flow cell was captured on a camera (PL-B781, Pixelink, Ontario, Canada) using an integration time of 25 ms. The image was converted to a 1D profile by integrating gray values along x-axis and plotting them as a function of pixel values along y-axis (where x- and y-axis refers to the position across the width of the device and angle of incidence respectively). The data on shift in peak position, which was estimated using a centre of gravity algorithm and a threshold of 60% of the height of the peak, was used to determine the refractive index sensitivity of MCLW devices.

Two-dimensional (2D) imaging was performed using the collimated beam emitted from the TE-polarised RCLED and the camera.  $2\ \mu\text{l}$  drops of different concentrations of glycerol solutions were placed on the MCLW and an output image was captured at angles of incidence in the range between  $60^\circ$  and  $80^\circ$ . The camera integration time was 25 ms. A plot of average gray value as a function of different concentrations of glycerol solutions was used to determine the refractive index sensitivity of the MCLW at a chosen angle of incidence. The spatial resolution of the MCLW was determined by probing devices constructed by depositing NOA 13685 on titanium rectangles of different sizes.

EWOD actuation was performed by applying a DC potential of  $\sim 80\ \text{V}$  between the electrodes on the lower and upper plates using a high voltage power supply (PS350, Stanford Research Systems, Hertfordshire, UK). The angle of incidence of the light source was fixed at  $68^\circ$  and the camera integration time was 25 ms. The movies were made using Windows movie maker and the frames were extracted via DVDVideoSoft.

### 3. Results and Discussion

#### 3.1. Preliminary study

Figure 2 (a) shows the profile of the optical mode travelling in the MCLW structure for TE-polarised light, which was obtained using a transfer matrix modelling package (L-Pro version 4.0).

The effect of spin coating speed of the NOA 13685 on the output curve of the MCLW device is shown in Figure 2 (b). The film thickness obtained by using spin speeds between 4000 rpm and 6000 rpm was close to cut-off for supporting an optical mode. At 1500 rpm, on the other hand, the NOA 13685 layer was comparatively non-uniform. As a result, devices consisting of NOA 13685 waveguide layer deposited at 2000 rpm were selected to perform the rest of the work.

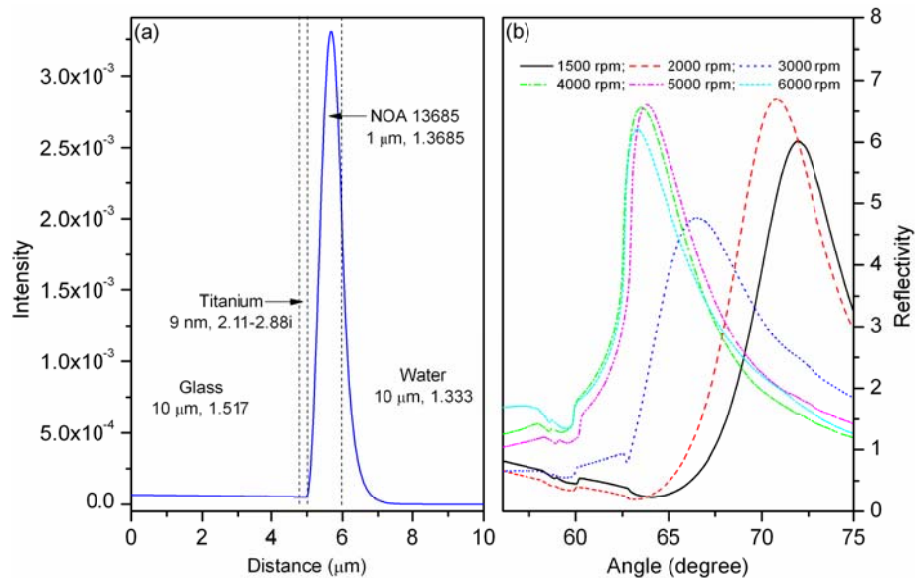


**Figure 2: Profile of the (a) optical mode obtained via modelling and (b) output of MCLW devices consisting of NOA 13685 spun at different speeds**

A typical image captured by the camera placed on the output side of the MCLW device and the shift in peak position *versus* time for different concentrations of glycerol solutions is shown in Figure 3. The relationship between the change in reflectivity peak position and the refractive index of glycerol solutions was linear and is given by  $\text{pixel} = -5644.9 + 4236.3 \times \text{refractive index}$  with  $r^2 = 0.983$ . Thus, the sensitivity of the RM device is 4236.3 pixels per refractive index unit (RIU).

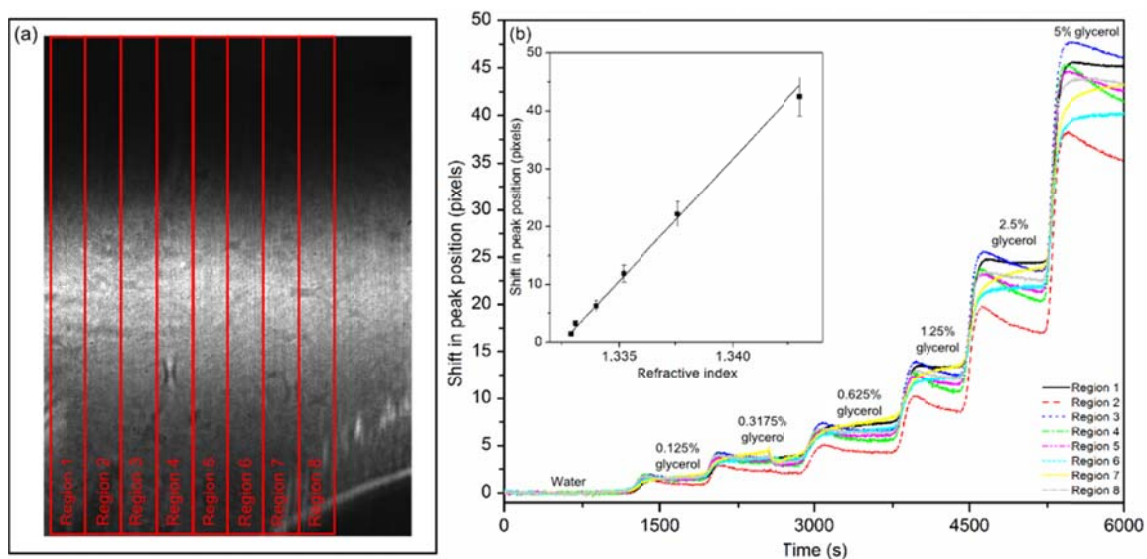


**Figure 3: (a) Typical output profile and (b) plot of shift in peak position *versus* time (where the inset shows refractive index sensitivity of the device)**

### 3.2. 2D imaging

The output of the MCLW with droplets of different concentrations of glycerol solutions at selected angles of incidence of the light source is shown in Figure 4 (a). As shown in Figure 4 (b), the normalised gray scale value decreases as the concentration (and hence the refractive index) of the droplet of glycerol solution increases at  $68^\circ$ . This is because the resonance angle of the MCLW increases as it is flushed with high concentrations of glycerol solutions. Similarly, the normalised gray scale value increases at the concentration of droplet of glycerol solution increases at  $77^\circ$ . Figure 7 (b) also shows that the sensitivity of detection of the MCLW device is highest at  $68^\circ$ . As a result, the angle of incidence of the light source was fixed at  $68^\circ$  in the rest of the work.

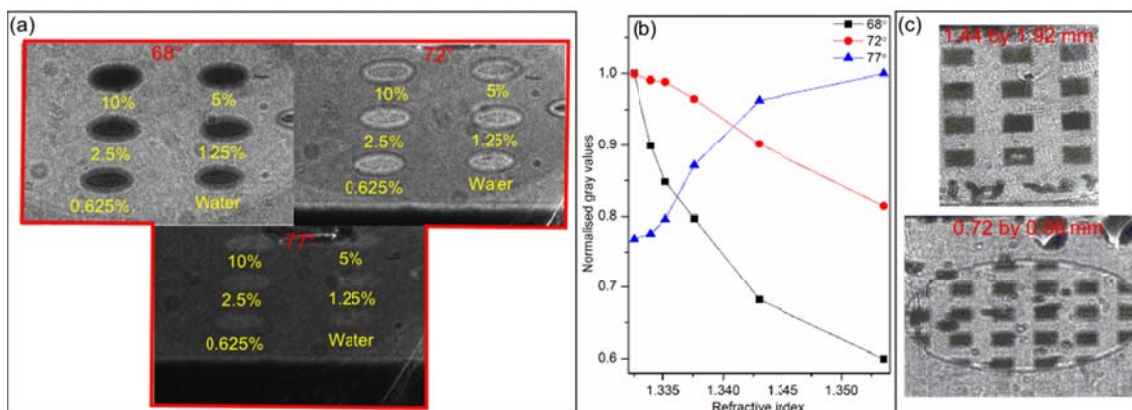


**Figure 4: (a) Output and (b) refractive index sensitivity of the MCLW with continuous titanium layer and (c) output of the MCLW with patterned titanium layer**

With the set-up currently used to probe the MCLW, devices consisting of titanium rectangles of  $0.72\text{ mm} \times 0.96\text{ mm}$  and  $1.44\text{ mm} \times 1.92\text{ mm}$  were successfully imaged (see Figure 4 (c)). The edges of titanium rectangles of size  $0.36\text{ mm} \times 0.48\text{ mm}$  were, however, blurred and could not be resolved using the current set-up. The spatial resolution of the MCLW can be enhanced by using a highly collimated non-coherent (to avoid laser speckle) beam emitted by for example, superluminescent diodes or a supercontinuum source.

### 3.3. MCLW integrated with EWOD

MCLW detection was then used to monitor the position of water droplet as a function of time on applying a potential between a top and bottom pair of electrodes (see Figure 5). The droplet moves between 0.5 and 1 seconds in Figure 5. The droplets appear elliptical because of foreshortening caused by the high angle between the EWOD device and the camera.

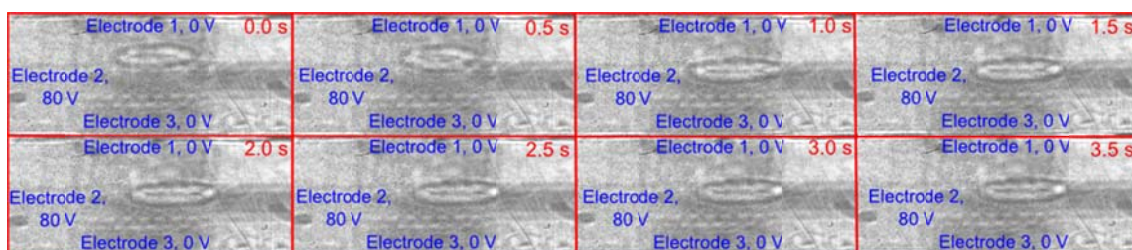


**Figure 5: Position of a water droplet monitored using MCLW within the EWOD device**

Subsequently, as shown in Figure 6, MCLW detection was shown to be suitable to monitor the mixing of two water droplets within an EWOD device. Future work will focus on increasing the spatial resolution of the MCLW detection by using highly collimated light sources. In addition, an

optimised electrode design will be used to lower the required actuation voltage. Finally, the suitability of the MCLW integrated EWOD device to solve real-world problems will be demonstrated.

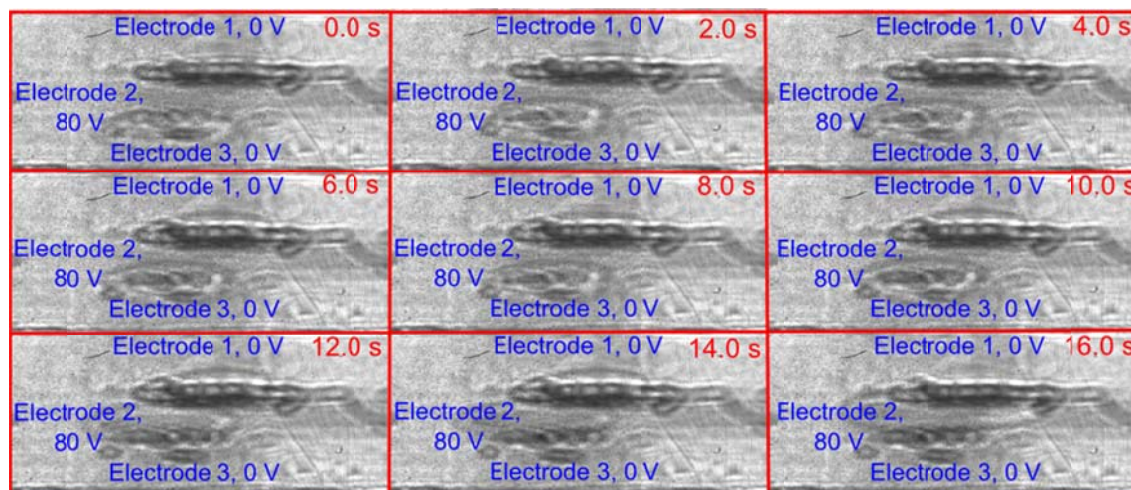


**Figure 6: Monitoring of mixing of two water droplets within the EWOD device via MCLW**

#### 4. Conclusions

Currently used optical techniques for detection within EWOD devices require "clean" samples, additional fabrication steps and complex integration. In order to address these issues, this work demonstrates the suitability of metal clad leaky waveguide (MCLW) for detection within EWOD.

MCLW sensing has been shown to be directly compatible with EWOD devices as the basic structure of both is the same. Preliminary work has shown that high optical quality hydrophobic films can be deposited on both continuous and patterned titanium layers and that these give reproducible responses to refractive index change. Both peak position monitoring with wedge beams and intensity monitoring using whole chip imaging with collimated light have been shown to be capable of detecting small changes in refractive index. In addition, water droplets have been imaged directly and their position monitored in real time. This real time capability was exploited to follow the movement of droplets and droplet merging under EWOD actuation.

#### References

- [1] I. Barbulovic-Nad, H. Yang, P.S. Park, A.R. Wheeler, *Lab Chip* 8 (2008) 519.
- [2] Y.-H. Chang, G.-B. Lee, F.-C. Huang, Y.-Y. Chen, J.-L. Lin, *Biomed. Microdevices* 8 (2006) 215.
- [3] M.J. Jebrail, A.H.C. Ng, V. Rai, R. Hili, A.K. Yudin, A.R. Wheeler, *Angew. Chem. Int. Ed.* 49 (2010) 8625.
- [4] V.N. Luk, A.R. Wheeler, *Anal. Chem.* 81 (2009) 4524.
- [5] R.S. Sista, A.E. Eckhardt, V. Srinivasan, M.G. Pollack, S. Palanki, V.K. Pamula, *Lab Chip* 8 (2008) 2188.
- [6] E.M. Miller, A.R. Wheeler, *Anal. Chem.* 80 (2008) 1614.
- [7] V. Srinivasan, V.K. Pamula, M.G. Pollack, R. Fair, in *MEMS, IEEE 16<sup>th</sup> International*, IEEE, Kyoto, Japan, 2003, p. 327.
- [8] L. Malic, T. Veres, M. Tabrizian, *Lab Chip* 9 (2009) 473.
- [9] C. Lerma Arce, D. Witters, R. Puers, J. Lammertyn, P. Bienstman, *Anal. Bioanal. Chem.* 404 (2012) 2887.
- [10] F. Ceyssens, D. Witters, T. Van Grimbergen, K. Knez, J. Lammertyn, R. Puers, *Sens. Act. B* 181 (2013) 166.
- [11] M. Zourob, N.J. Goddard, *Biosens. Bioelectron.* 20 (2005) 1718.
- [12] R. Gupta, B. Bastani, N.J. Goddard, B. Grieve, *Analyst* 138 (2013) 307.